2012 IEEE International Conference on Robotics and Automation
RiverCentre, Saint Paul, Minnesota, USA
May 14-18, 2012

Automated Throwing and Capturing of Cylinder-Shaped Objects

Thorsten Frank, Uwe Janoske, Anton Mittnacht and Christian Schroedter

***Abstract*—A new approach for transportation of objects within production systems by automated throwing and capturing is investigated. This paper presents an implementation, consisting of a throwing robot and a capturing robot. The throwing robot uses a linear and the capturing robot a rotary axis. The throwing robot is capable of throwing cylinder-shaped objects onto a target point with high precision. The capturing robot there smoothly grips the cylinders during flight by means of a rotational movement. In order to synchronize the capturing robot and the cylinder's pose and velocity, its trajectory has to be modeled as well as the motion sequences of both robots. The throwing and capturing tasks are performed by the robots automatically without the use of any external sensor system.**

I. Introduction

In order to remain competitive the performances of factories, such as throughput rates or cycle times, have to be improved continuously. Processes have to be designed to a maximum of efficiency without suffering loss of flexibility in consideration of shortened product lifecyles and increasing product variants. In this context, also in-plant transportation is to be considered by factory planners.

At Heilbronn University a new approach is investigated, which considers transportation of objects within production systems by automated throwing and capturing. The potentials of this approach have already been described in [1], [2]. In this paper, a prototype implementation is presented which is capable of automatically throwing and capturing of cylinder-shaped objects with varying masses and geometric dimensions. A single-degree-of-freedom (1-DOF) throwing robot accelerates the cylinders in their axial direction by a linear axis and another 1-DOF robot, which consists of a rotary axis and a gripper, captures them smoothly by a rotational movement. Therefore, at the capturing point the movement of the gripper on the capturing robot must be aligned to the pose and velocity of the flying cylinder (Fig. 1).

Manuscript received July 20, 2011. This work was supported by the Foundation for the Promotion of the Reinhold-Wuerth-University of the Heilbronn University.

T. Frank is with the Heilbronn University, Campus Kuenzelsau - Reinhold-Wuerth-University, Daimlerstrasse 35, 74653 Kuenzelsau, Germany (phone: +49-7940/1306-145; email: thorsten.frank@hs-heilbronn.de).

U. Janoske is with the University of Wuppertal, Institute of Fluid Mechanics, Gaussstrasse 20, 42119 Wuppertal, Germany (email: janoske@uni-wuppertal.de).

A. Mittnacht is with the Heilbronn University, Campus Kuenzelsau - Reinhold-Wuerth-University, Daimlerstrasse 35, 74653 Kuenzelsau, Germany (email: mittnacht@hs-heilbronn.de).

C. Schroedter is with the Heilbronn University, Campus Kuenzelsau - Reinhold-Wuerth-University, Daimlerstrasse 35, 74653 Kuenzelsau, Germany (email: schroedter@hs-heilbronn.de).

II. State-of-the-art

Meanwhile, throwing of balls by robots has been investigated in numerous approaches. Serial robots with rotary axis are frequently used [3, 4, 5, 6, 7]. In [7], for instance, a robot is described which is capable of throwing balls into a moving basket with a success rate of 99%. However, these robots usually impose a torque on axial thrown cylinder-shaped objects, leading to an unstable flight and thereby complicating the capturing process.

In [8], a gantry robot is proposed which captures balls, thrown by humans, with a success rate of 66%.

Capturing of cylinder-shaped objects, however, implicates the consideration of not only the position but also the orientation. Robotic grasping of totally unordered but stationary cylinders in a bin is described in [9]. In [10] a robotic hand is introduced, which is capable of capturing falling cylinders. A robotic hand which slightly throws up a cylinder and afterwards captures it by dynamic regrasping with a success rate of 35% is presented in [11].

All approaches mentioned beforehand use vision systems, which measure the pose of the objects. The approach presented in this paper, however, eliminates the necessity of external sensors using a holistic model of the thrown cylinder's trajectories to which the robot's motion sequences are adapted. Such a system, consisting of two robots capable of throwing and smoothly capturing of cylinder-shaped objects over a distance of 3 m, has not been reported so far.

III. Trajectories of Thrown Cylinders

We already described trajectories of thrown cylinder-shaped objects in [12]. Fig. 2 depicts the trajectory of a compliantly flying cylinder. Here, the orientation of the cylinder follows more or less precisely its speed vector. This compliance is caused by the physical effects of shoulder stabilization [13] and arrow stabilization [14].

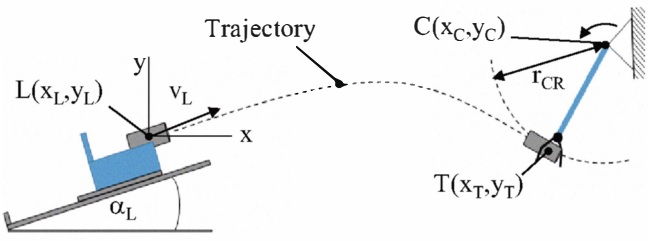

Fig. 1. Basic concept

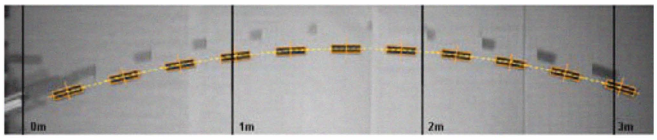

Fig. 2. Trajectory of a compliantly flying cylinder

Particularly, shoulder stabilization has a significant effect for cylinders with a plane frontside not too small in size. Arrow stabilization is caused by an unsymmetrical mass distribution within the cylinder.

According to [12], different models which enable the simulation of trajectories for point masses can be applied to compliantly flying cylinders. For those cylinders, the positions $\underline{r}$ and the velocities $\underline{v}$ on trajectories can be calculated according to (1) and (2) [15].

$$\underline{r}_{k+1} = \begin{pmatrix} x_k + \Delta t \cdot v_{x,k} \\ y_k + \Delta t \cdot v_{y,k} \end{pmatrix} \tag{1}$$

$$\underline{v}_{k+1} = \begin{pmatrix} v_{x,k} - \Delta t \cdot \left(\frac{K}{m} \cdot v_{x,k} \cdot \sqrt{v_{x,k}^2 + v_{y,k}^2} \right) \\ v_{y,k} - \Delta t \cdot \left(g + \frac{K}{m} \cdot v_{y,k} \cdot \sqrt{v_{x,k}^2 + v_{y,k}^2} \right) \end{pmatrix} \tag{2}$$

In these equations, Δt is the step of the numerical evolution of the trajectory, m represents the mass of the cylinder and the constant K is calculated as

$$K = c_D \cdot \frac{\rho}{2} \cdot A \tag{3}$$

Hereby, ρ is the ambient density, c_D is the drag factor and the cross-section area is given by $A = \pi \cdot r_{Cyl}^2$. The value r_{Cyl} represents the radius of the cylinder. The corresponding initial conditions for the approach according (1) and (2) are determined as

$$\underline{r}_{k+1} = \begin{pmatrix} 0 \\ 0 \end{pmatrix}; \underline{v}_{k+1} = \begin{pmatrix} v_L \cdot \cos\alpha \\ v_L \cdot \sin\alpha \end{pmatrix} \tag{4}$$

where v_L is the launching velocity and α_L represents the launching angle. For an ideally compliantly flying cylinder, the orientation of the cylinder along the whole trajectory always equals the angle of trajectory α_k. This angle is given at each point on the trajectory by

$$\tan\alpha_k = \frac{v_{y,k}}{v_{x,k}}. \tag{5}$$

IV. Experimental Setup

A. Throwing robot

This paper describes throwing of cylinders by a linear axis (Fig. 3a). A servomotor (Siemens 1FK7) drives a tooth belt which moves a carriage. The cylinders to be thrown are put onto this carriage. Throwing is performed by accelerating and then decelerating the carriage. The servomotor is equipped with an absolute angular encoder with a precision of ±0.01°. This enables an accurate indirect measurement of the position and the velocity of the carriage.

B. Capturing robot

As mentioned before, the capturing of cylinders is performed by 1-DOF robot as well (Fig. 3b). Its rotary axis is also actuated by a Siemens 1FK7 servomotor. The axis is connected to the motor by an angular gear with a transmission ratio of 7:1. The end effector is a pneumatic gripper LGW25 from Schunk which is mounted on a lever arm. This gripper achieves a closing time of approximately 10 ms.

C. Control

Both the throwing robot and the capturing robot are controlled by a common Siemens SIMOTION motion control system. For each one, this system provides a cascade controller for current, motor speed and position. It can be programmed with the Structured Control Language (SCL). Communication between control and drives is put into effect by Drive-Cliq.

V. Model for Throwing and Capturing

A. Determination of Launching Parameters

In case of throwing and capturing objects for in-plant transportation, the launching point L and the capturing point T can be assumed to be known. For capturing a cylinder by a rotary axis, the cylinder's trajectory has to meet the end effector's circular trajectory in T tangentially (Fig. 1). Therefore, the orientation of the gripper and, thus, the orientation of the compliantly flying cylinder at point T can be calculated as

$$\tan\alpha_T = \frac{x_C - x_T}{y_T - y_C}. \tag{6}$$

Hereby, x_C and y_C are the coordinates of the rotary axis. As presented in [12], for compliantly flying cylinders, there exists only one combination of values for v_L and α_L, which leads to a trajectory on which the cylinder reaches the capturing point in a predefined pose. We presented an algorithm for the determination of the launching parameters v_L and α_L in [12] as well.

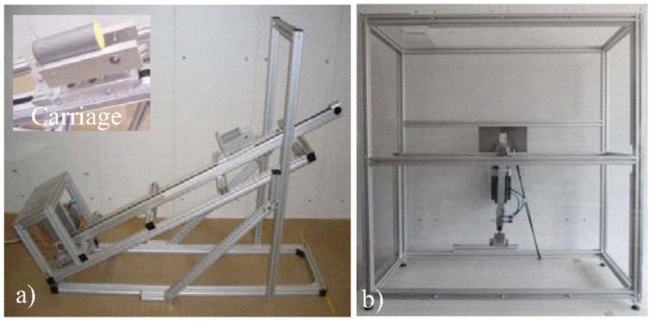

Fig. 3. Two Robots: a) Throwing Robot, b) Capturing Robot

B. *Throwing Model*

The basic sequence for throwing a cylinder with a linear axis is shown in Fig. 4. It consists of three steps (Fig. 5):

- Step 0-1: The carriage is accelerated up to a position $s_{1,Com}$.
- Step 1-2: At the $s_{1,Com}$ position, the deceleration of the carriage is initiated. Because of an inevitable delay between command values and actual values, it takes the time t_{12} from t_1 to t_2 until the carriage really decelerates.
- Step 2-3: The carriage is decelerated. Because of the inertia of the cylinder and provided there is low friction, it continues to move with nearly the maximum speed $v_{2,Act}$ which was achieved by the carriage. The cylinder starts its flight, when its center of gravity leaves the carriage at $t_3 = t_{Throw}$.

Obviously, it has to be ensured, that, at launching point (position s_{Throw} vs. time t_{Throw}), the cylinder meets the necessary launching parameters v_L and α_L as described in section A. Therefore, the command position $s_{1,Com}$ and the command acceleration $a_{01,Com}$ have to be calculated in a backward direction from t_{Throw}. For this, the following parameters are given:

- launching velocity (v_L)
- launching angle (α_L),
- deceleration of carriage ($a_{23,TR}$),
- shift-distance of the cylinder on the carriage ($\Delta s_{23,Cyl\text{-}TR}$).

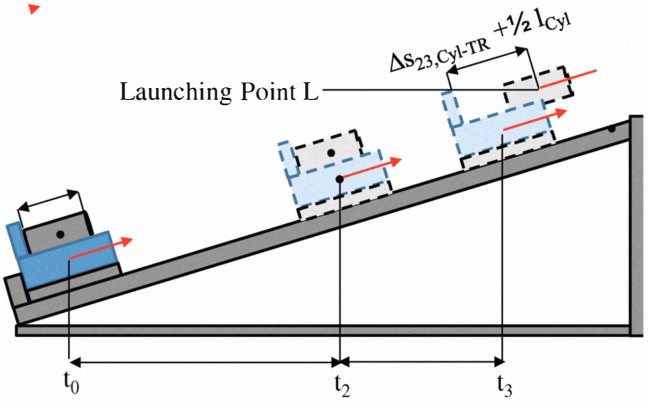

Fig. 4. Motion sequence of throwing robot. The time steps t_0, t_2 and t_3 correspond to the time steps in Fig. 5.

During step 2-3, the cylinder is slightly decelerated due to friction, air drag and grade resistance. This deceleration can be approximated by

$$a_{23,Cyl} = g \cdot \cos\alpha_L + \frac{c_D \rho A v_{3,Act}^2}{2m} + \frac{\mu F_N}{m} \qquad (7)$$

where μ is the friction coefficient and F_N is the normal force. The covered distances of the carriage $s_{23,Act,TR}$ and of the cylinder $s_{23,Cyl}$ during step 2-3 is calculated as

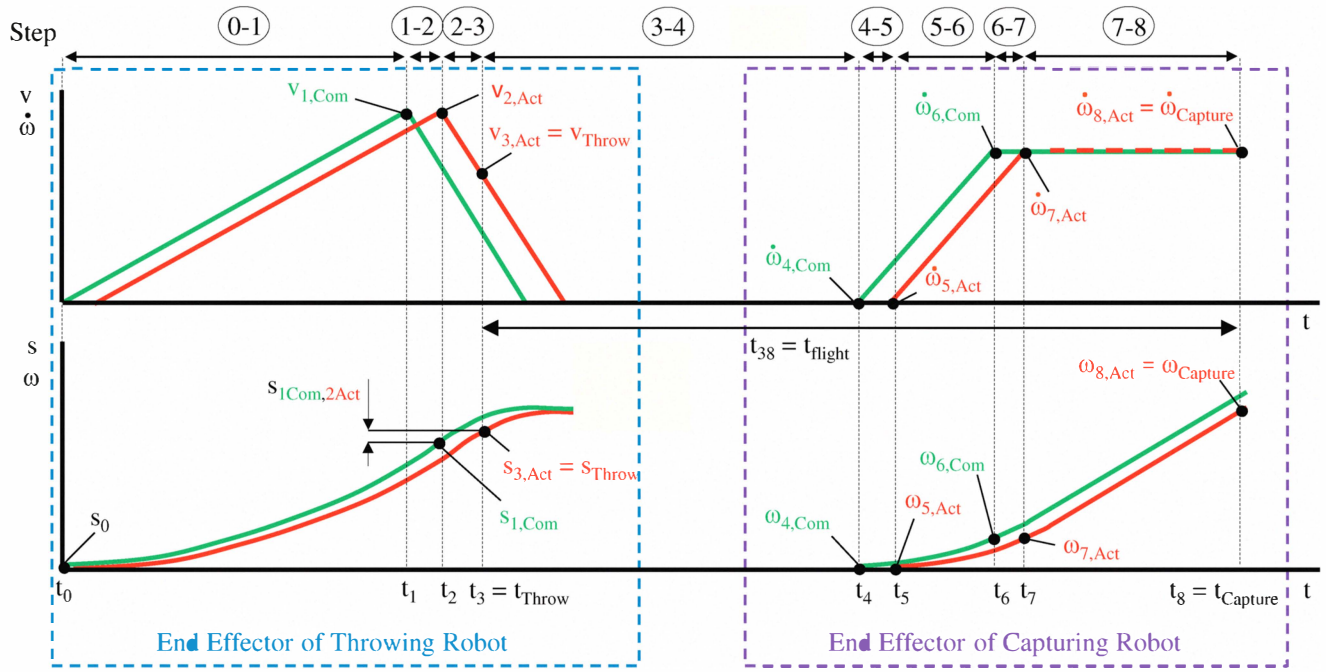

Fig. 5. Positions and velocities of the robot in the procedural sequence of throwing and capturing. The index "Com" points out the command values; "Act" refers to actual values. One subscripted number denotes an absolute variable at the corresponding point of time; e.g. s_1 is the absolute position at point of time t_1. Two subscripted consecutive numbers represent a relative variable between the corresponding point of times; e.g. $s_{23} = s_3 - s_2$ is the relative position at t_3 regarding t_2.

$$s_{23,Cyl} = v_{2,Cyl} t_3 + \frac{1}{2} a_{23,Cyl} t_{23}^2; \quad (8)$$

$$s_{23,Act,TR} = v_{2,Act,TR} t_3 + \frac{1}{2} a_{23,TR} t_{23}^2. \quad (9)$$

The duration of step 2-3 t_{23} can be calculated with the relative distance between $s_{23,Cyl}$ und $s_{23,Act,TR}$ which is at t_{Throw} equal to $\Delta s_{23,Cyl\text{-}TR}$:

$$t_{23} = \sqrt{\frac{2 \cdot \Delta s_{23,Cyl-TR}}{a_{23,TR} - a_{23,Cyl}}} \quad (10)$$

Consecutively $v_{1,Com}$ which is equal to $v_{2,Act}$ is given by the following equation:

$$v_{1,Com} = v_{2,Act} = v_L + a_{23,Cyl} \cdot t_{23}^2 \quad (11)$$

Thus, the required variables for controlling the throwing robot $s_{1,Com}$ and $a_{01,Com}$ yield

$$s_{1,Com} = s_{Throw} - s_{1Com,2Act} - s_{23,Act}; \quad (12)$$

$$a_{01,Com} = \frac{v_{1,Com}^2}{2 \cdot s_{1,Com}}. \quad (13)$$

In (12), there exists no analytical solution for the distance $s_{1Com,2Act}$. Therefore, a simulation, which considers the feedback control of the robot axis, is required. This issue is considered in section D.

In order to enable the interaction between both robots, the time of throwing t_{Throw} has to be identified. Therefore, t_1 is calculated as

$$t_1 = \frac{2 \cdot v_{1,Com}^2}{a_{01,Com}}. \quad (14)$$

Thus, t_{Throw} is given by

$$t_{Throw} = t_1 + t_{12} + t_{23}. \quad (15)$$

Calculation of t_{12}, is again performed by the simulation, introduced in section D.

C. Capturing Model

As denoted in chapter IV, the capturing robot must grab the thrown cylinder smoothly during a rotational movement. Therefore, the robot must be accelerated timeously to the velocity of the cylinder at the capturing point. With the model for trajectories of compliantly flying cylinders described in chapter III the velocity of the flying cylinder at the capturing point v_T can be calculated as well as the time t_{flight} elapsed from launching point to the capturing point. Thus, the angular velocity $\dot{\omega}_{Capture}$ of the capturing robot at the capturing point can be determined as

$$\dot{\omega}_{Capture} = \frac{180 \cdot v_{Capture}}{\pi \cdot r_{CR}} \quad (16)$$

Here, r_{CR} represents the length between the robot's rotary axis and its tool center point (TCP) (Fig. 1). The time of capturing $t_{Capture}$ can be calculated as

$$t_{Capture} = t_{Throw} + t_{Flight}. \quad (17)$$

The required time for the acceleration of the rotary axis t_{46} and the corresponding covered angular distance $\omega_{46,Com}$ can be calculated according to (18) and (19).

$$t_{46} = \frac{\dot{\omega}_{Capture}}{\ddot{\omega}_{46,Com}} \quad (18)$$

$$\omega_{46,Com} = \frac{1}{2} \ddot{\omega}_{46,Com} t_{46}^2. \quad (19)$$

It should be noted that in the model t_{46} is equal to t_{57} and $\omega_{46,Com}$ is equal to $\omega_{57,Act}$. At t_{46}, the angular acceleration $\ddot{\omega}_{46,Com}$ is pre-defined and has to fulfill the following condition:

$$\ddot{\omega}_{46,Com} < \frac{2\omega_{Capture}}{t_{58}^2} \quad (20)$$

Thus, the angular distance $\omega_{78,Act}$ as well as the corresponding elapsed time t_{78} is calculated as

$$\omega_{78,Act} = \omega_{Capture} - \omega_{5,Act} - \omega_{57,Act}; \quad (21)$$

$$t_{78} = \frac{\omega_{78,Act}}{\dot{\omega}_{78,Act}}. \quad (22)$$

$\omega_{5,Act}$ represents the predefined initial angular position of the capturing robot. The elapsed time t_{68} is thus given by

$$t_{68} = t_{67} + t_{78}. \quad (23)$$

Notably t_{67} has to be determined by the simulation of the feedback control of the axis which is described in section D. Finally, the acceleration time t_4 is given by

$$t_4 = t_{Capture} - t_{68} - t_{46}. \quad (24)$$

A timer is activated when the throwing robot's end effector passes the position s_{Throw}. When the time $t_{24} = t_4 - t_{Throw} + t_{23}$ is elapsed, the capturing robot accelerates.

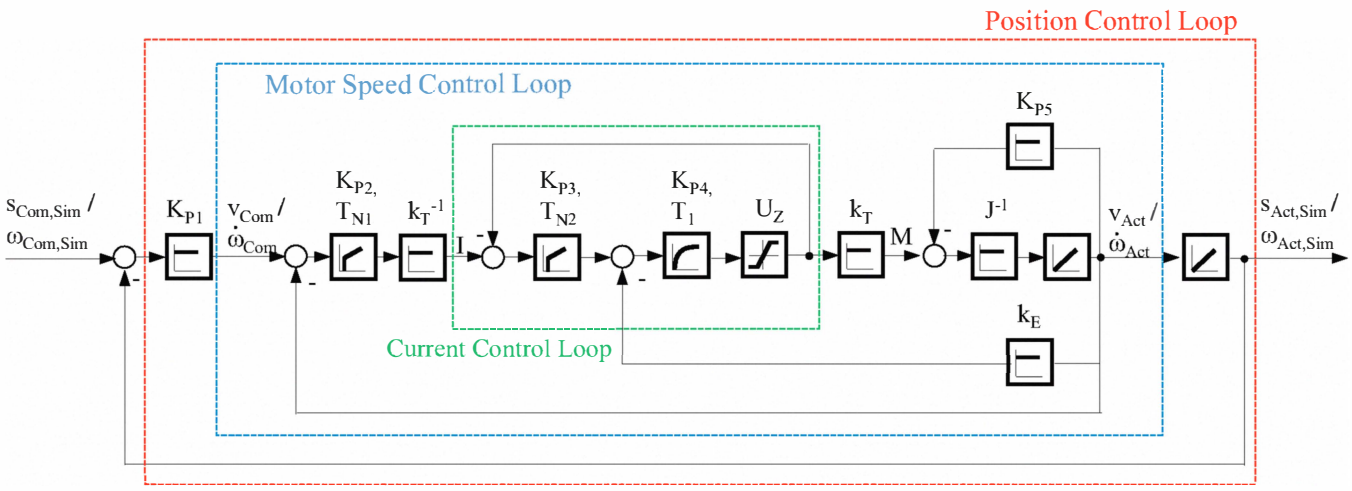

K_{P1}: Proportional Gain of Position Controller
K_{P2}: Proportional Gain of Motor Speed Controller
T_{N1}: Reset Time of Motor Speed Controller
k_T: Torque Constant
I: Current
K_{P3}: Proportional Gain of Current Controller
T_{N2}: Reset Time of Current Controller
K_{P4}: Proportional Gain of Command Value Filter
T_1: Time Constant of Command Value Filter
M: Turning Moment
U_Z: Intermediate Circuit Voltage
J: Moment of Inertia incusive Load
K_{P5}: Proportional Gain due to Friction
k_E: Voltage Constant

Fig. 6. The control system diagram of a robot axis

D. Model for Feedback Control

As described in sections B and C, the parameters $s_{1Com,2Act}$, t_{12} and t_{67} must be determined in order to model the holistic procedure of throwing and capturing. According to Fig. 4, these parameters specify deviations between command values and their actual values. The calculation of these parameters can be performed by simulating the robot's position and velocity control. Both robots are actuated by servomotors. For these kinds of motors, models for feedback control are already available. In this paper, a model as described in [16] has been adapted for the throwing and capturing robot. The corresponding block diagram for both robots is illustrated in Fig. 6. For the simulation, the interpolation of the command position $s_{Com,Sim,TR}$ of the linear axis is performed with (25).

$$s_{Com,Sim,TR} = \begin{cases} \dfrac{v_{1,Com}^2}{\left(s_{Throw} - s_{23,Act,TR}\right)} t^2, t \le \dfrac{2\left(s_{Throw} - s_{23,Act,TR}\right)}{v_{1,Com}} \equiv t^* \\ \dfrac{v_{1,Com}^2}{s_{Throw} - s_{23,Act,TR}} t^{*2} + v_{1,Com}(t - t^*) \\ \quad + \dfrac{1}{2} a_{23,Act,TR}(t - t^*)^2, \qquad t^* < t \end{cases} \tag{25}$$

Correspondingly, the interpolation of the command position $\omega_{Com,Sim,TR}$ of the rotary axis is performed with (26).

$$\omega_{Com,Sim,CR} = \begin{cases} 0, & t < t_8 - t_{46} - t_{78} \equiv t^{**} \\ \dfrac{1}{2}\ddot{\omega}_{46,Com}(t - t^{**})^2, & t^{**} \le t \le t^{**} + t_{46} \equiv t^{***} \\ \dfrac{1}{2}\ddot{\omega}_{46,Com}(t^{***} - t^{**})^2 + v_{6,Com}(t - t_6), & t^{***} < t \end{cases} \tag{26}$$

VI. Experimental Validation

In a series of experiments, the feasibility of automated throwing and capturing of cylinders has been validated.

The cylinder's mass was m = 34 g; its radius was r_{Cyl} = 0.02 m and its length l = 0.1 m. The flight of the cylinder showed good compliancy and, thus, good flight stability.

The capturing robot's rotary axis was positioned in a distance of x = 3 m from launching point. The length between the robot's rotary axis and its TCP was r_{CR} = 0.472 m and the end effector's orientation at capturing point was set to α_T = -20.9°.

The launching parameters were thus calculated as v_L = 6.6 m/s and α_L = 26°. According to the model for trajectories described in chapter III, the time of flight was t_{flight} = 492.9 ms.

The deceleration of the carriage $a_{23,TR}$ was set to 150 m/s^{2}and the shift-distance of the cylinder on the carriage was $\Delta s_{23,Cyl\text{-}TR}$ = 0.1 m. The initial position of the capturing robot was 90°. The robot was accelerated by $\ddot{\omega}_{46,Com}$ = 4000°/s^2.

With these values, the sequence for throwing and capturing of the cylinder could be simulated by the model described in Section V using Matlab Simulink. Thus, the capturing robot had to be accelerated with the time interval

of t_{34} = 174 ms after the cylinder was thrown.

Adjusting the parameters, fifty throws were performed in this series of experiments. The success rate for capturing the cylinders was 100 %. In these experiments, the command values and actual values for the positions and velocities of both robot axes were also recorded within the SIMOTION. So they could be compared with the corresponding values which were achieved by the simulation (Fig. 7.). Fig. 8 shows an image sequence, presenting the capturing of the cylinder.

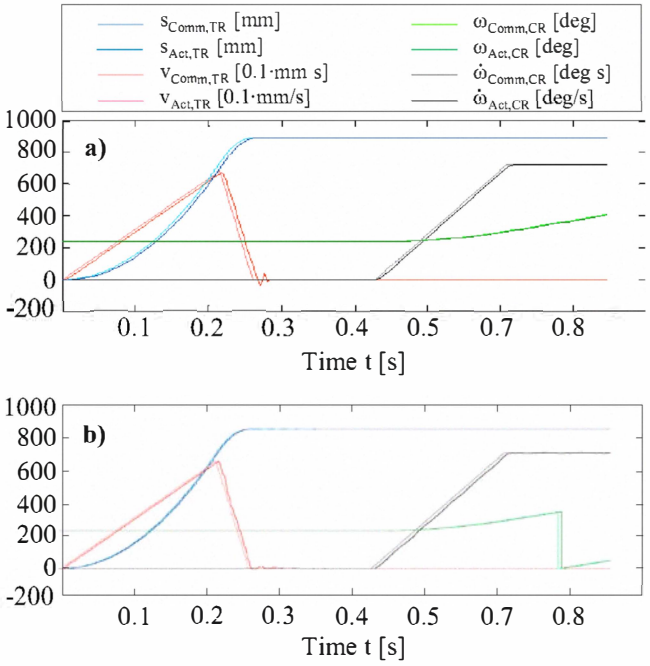

Fig. 7. Position and velocity as a function of time a) Simulation results, b) Measurement Results

VII. Conclusion

A system, consisting of two robots has been developed for throwing and smooth capturing of cylinder-shaped objects. A model has been developed, which enables the calculation of the sequences of this system. With this model, the robots can be controlled. In a series of experiments, throws of a cylinder with good flight stability have been captured with a success rate of 100%. In the future a capturing robot is to be developed which is capable of capturing instable flying cylinders. Therefore, the robot has to be equipped with an additional sensor system which measures the cylinder's pose during flight and controls the end-effector to the corresponding capturing pose.

Acknowledgment

The authors thank Schunk GmbH & Co. KG for consultancy and cooperation. Particularly, the design and manufacturing of the high performance gripper was a valuable contribution to this research.

References

[1] Frank, H., "Throwing of Objects: A New Technology for Factory Automation," Computational Intelligence, Communication Systems and Networks, 2009. CICSYN '09. First International Conference on , vol., no., pp.4-5, 23-25 July 2009

[2] Frank, H.; Wellerdick-Wojtasik, N.; Hagebeuker, B.; Novak, G. and Mahlknecht, S.; , "Throwing Objects -- A bio-inspired Approach for the Transportation of Parts," Robotics and Biomimetics, 2006. ROBIO '06. IEEE International Conference on , vol., no., pp.91-96, 17-20 Dec. 2006

[3] Senoo, T.; Namiki, A. and Ishikawa, M., "High-speed throwing motion based on kinetic chain approach," Intelligent Robots and Systems, 2008. IROS 2008. IEEE/RSJ International Conference on , vol., no., pp.3206-3211, 22-26 Sept. 2008

[4] Lombai, F. and Szederkenyi, G., "Throwing motion generation using nonlinear optimization on a 6-degree-of-freedom robot manipulator," Mechatronics, 2009. ICM 2009. IEEE International Conference on , vol., no., pp.1-6, 14-17 April 2009

[5] Gams, A.; Petric, T.; Zlajpah, L. and Ude, A., "Optimizing parameters of trajectory representation for movement generalization: robotic throwing," Robotics in Alpe-Adria-Danube Region (RAAD), 2010 IEEE 19th International Workshop on , vol., no., pp.161-166, 24-26 June 2010

[6] Shoji, T.; Nakaura, S. and Sampei, M., "Throwing motion control of the springed Pendubot via unstable zero dynamics," Control Applications (CCA), 2010 IEEE International Conference on , vol., no., pp.1602-1607, 8-10 Sept. 2010

[7] Hu, J - S.; Chien, M. . C.; Chang, Y. - J; Su, S. – H. and Kai, C. – Y., "A ball-throwing robot with visual feedback," Intelligent Robots and Systems (IROS), 2010 IEEE/RSJ International Conference on , vol., no., pp.2511-2512, 18-22 Oct. 2010

[8] Barteit, D., "Tracking of Thrown Objects - Catching of mechanically thrown parts for transport in manufacturing," Dissertation, Vienna University of Technology, 2009.

[9] Stotz, M.; Kühnle, J. and Verl, A., "A novel approach to object recognition and localization in automation and handling engineering," in SPIE: Optomechatronic Technologies 2008: 17-19 November 2008, San Diego, California, USA. Bellingham, USA: SPIE - The International Society for Optical Engineering, 2008.

[10] Imai, Y.; Namiki, A.; Hashimoto, K. and Ishikawa, M., "Dynamic active catching using a high-speed multifingered hand and a high-speed vision system," Robotics and Automation, 2004. Proceedings. ICRA '04. 2004 IEEE International Conference on , vol.2, no., pp. 1849- 1854 Vol.2, April 26-May 1, 2004

[11] Furukawa, N.; Namiki, A.; Taku, S. and Ishikawa, M., "Dynamic regrasping using a high-speed multifingered hand and a high-speed vision system," Robotics and Automation, 2006. ICRA 2006. Proceedings 2006 IEEE International Conference on , vol., no., pp.181-187, 15-19 May 2006

[12] Frank, T.; Schroedter, C. and Janoske, U., "Holistic Modeling of Trajectories for Cylinder Shaped Objects," UKSim 4th European Modeling Symposium on Mathematical Modeling and Computer Simulation, 17-19 November 2010.

[13] Sellier, K. and Knuebuehl, P., "Wound ballistics and the scientific background," Elsevier Health Sciences, 1994.

[14] Badior, A., "Weiter Wurf – Ein Überblick über die Geschichte der äußeren Ballistik in Europa", APL – Journal, Berlin, Rhombos, 2004

[15] Gross, D.; Hauger, H. and Wriggers, P., "Technische Mechanik," Bd. 4. Sixth edition, Springer, 2007.

[16] Zirn, O. and Weikert, S., "Modellbildung und Simulation hochdynamischer Fertigungssysteme – Eine praxisnahe Einführung, Springer, 2006.

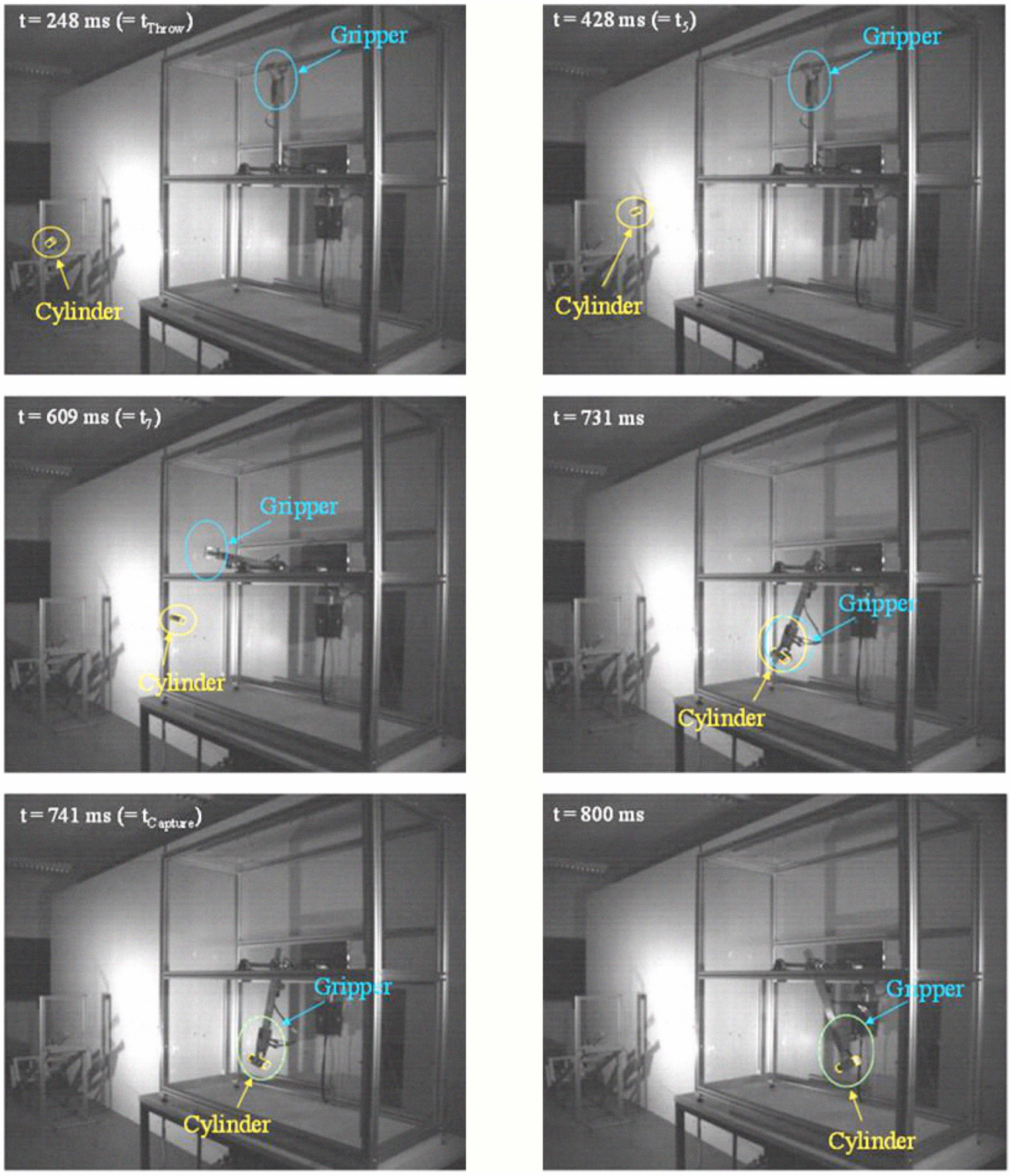

Fig. 8. Capturing of a thrown cylinder